

Fine structure in high-resolution photoemission spectra of quasi-two-dimensional 1T-TaS₂

Th. Pillo,^{1,*} J. Hayoz,¹ D. Naumović,¹ H. Berger,² L. Perfetti,² L. Gavioli,^{2,3} A. Taleb-Ibrahimi,³ L. Schlapbach,¹ and P. Aebi¹

¹*Institut de Physique, Université de Fribourg, CH-1700 Fribourg, Switzerland*

²*Institut de Physique Appliquée, EPF, CH-1015 Lausanne, Switzerland*

³*LURE, Centre Universitaire de Paris-Sud, F-91898 Orsay, France*

Using high-resolution angle-resolved photoemission spectroscopy (ARPES), we examined the charge density wave (CDW) compound 1T-TaS₂ as a function of the photon energy (energy range from 11 up to 33 eV) for both quasicommensurate (QC) and commensurate (C) CDW phases. While the QC-phase normal emission ARPES spectra coincide with previous results, normal emission spectra of the C phase reveal evidence for a fine structure in the CDW-induced features between 1 eV binding energy and the Fermi level. This fine structure may be explained by the subband manifold of the Ta 5*d* band, split off due to the CDW-induced $\sqrt{13} \times \sqrt{13}$ superstructure.

The layered transition-metal dichalcogenide (TMC) 1T-TaS₂ received much attention during the past three decades,¹⁻³ because it is one of the materials whose structural properties seem rather simple, whose electronic properties, however even today, are not yet fully understood.⁴ The reason for that is based on the presence of charge density waves (CDW's), occurring in several phases as a function of temperature. The lattice undergoes a periodic distortion (PLD) with a $\sqrt{13} \times \sqrt{13}$ symmetry.¹ This superlattice is incommensurate (IC) in the temperature region from 550 K to 350 K, quasicommensurate (QC) from 350 K to 180 K upon cooling (upon warming there is a hysteresis and the transition temperature is 230 K), and finally commensurate (C) below 180 K.^{1,3} The C phase is characterized by a totally locked-in CDW, which results in a rotation by 13.9° of the superlattice with respect to the Ta basal plane.⁵

As shown in Fig. 1(a), the particularity of the $\sqrt{13} \times \sqrt{13}$ superlattice is the fact that 13 Ta atoms form so-called "David" stars, forming two outerlying shells of 6 Ta atoms each and a centered 13th Ta atom. It is only this star-centered atom which contributes to conductivity as the outerlying shells form bonding orbitals. This model, first introduced by Fazekas and Tosatti⁶ (FT), predicts also a Mott transition,⁷ where the star-centered electron becomes susceptible to localization, resulting in a pseudogap over most of the Fermi surface (FS). On the other hand, FS nesting, as a possible mechanism driving the CDW transition, has not been observed explicitly in the regions around the *M* points,^{8,9} where it would be expected. However, the superstructure-mediated symmetry change gives rise to spectral fine structures whose existence has been partially proved by angle-resolved photoelectron spectroscopy (ARPES),⁸⁻¹⁵ especially around the Γ point,^{10,11} but also away from high-symmetry directions.^{8,9,12-15} A tight-binding calculation based on the FT model predicted the existence of CDW-related structures in ARPES spectra,¹³ including a certain intrinsic fine structure due to the removal of the degeneracy. This calculation is reproduced in Fig. 1(b). To our knowledge, only three CDW-related features could clearly be identified up to now, whereas the inherent fine structure of the CDW-induced bands could not be evidenced by ARPES data. Consequently,

the aim of this work is to present the predicted fine structure in the CDW-related spectral features along the perpendicular direction [ΓA] and at low temperatures (deep in the C phase).

Experiments were carried out at the French-Swiss beamline SU3 at SuperACO (LURE, Paris). This undulator beamline is equipped with a plane grating monochromator and the energy analysis of the photoelectrons was performed using a HAC 150 VSW hemispherical analyzer, yielding a combined energy resolution (photons and electrons) of 25 meV in the photon energy region used (11–33 eV). The angular resolution was $\pm 1^\circ$.

Pure samples of 1T-TaS₂ were prepared by chemical vapor transport.¹⁶ They were cut with a blade to the desired shape and glued with silver epoxy onto an Al platelet, which was mounted on a Cu sample spade. The sample orientation was controlled *ex situ* by x-ray diffraction. After that samples were transferred into UHV and cleaved *in situ*, yielding clean surfaces with the known $\sqrt{13} \times \sqrt{13}$ spots from the QC phase as checked by low-energy electron diffraction (LEED) at 300 K.

Measurements were performed at two temperatures: In the QC phase at 300 K and, using a He flow cryostat, at 20 K, i.e., far below the QC-C transition at 180 K. All spectra are normalized to the photon flux and the Fermi level of the experiment was calibrated, at all photon energies used, on freshly evaporated gold films deposited onto the measured surface.

In an ionic picture each of the Ta atoms [Fig. 1(a)] carries one electron. Two sets of six electrons each form then two shells (denoted 2 and 3 in Fig. 1). They represent molecular bonding orbitals and carry 12 out of the 13 electrons. These 12 electrons form hence 6 (2×3) filled electron bands, which are degenerate on each shell. The one electron left forms a half-filled band. This 13th electron constitutes the star center and is susceptible to localization giving rise to the Mott transition at 180 K. In part (b) of Fig. 1, we reproduce a tight-binding calculation performed by Smith *et al.*,¹³ which was based on band structure calculations of the undistorted phase, but now accounting for both the atomic displacements of the Ta atoms induced by the CDW formation

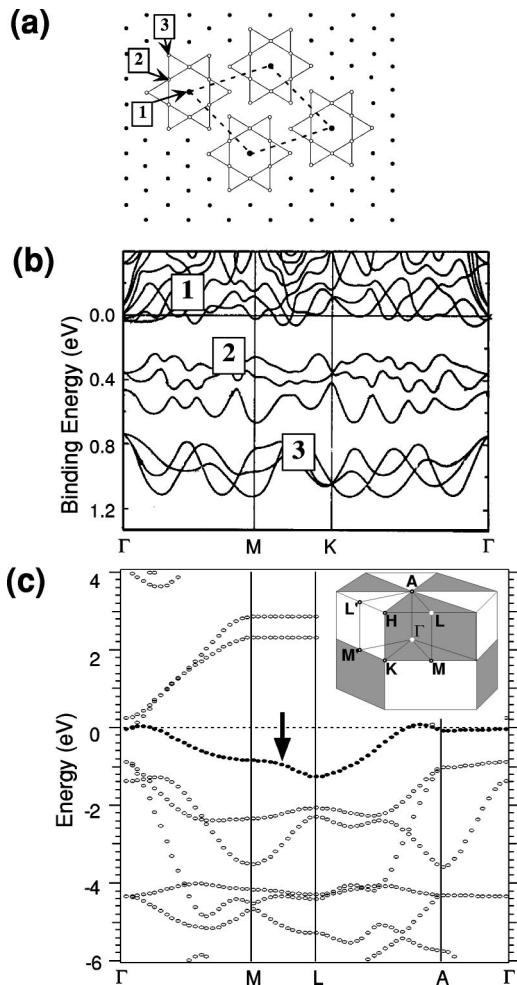


FIG. 1. (a) Schematic view of the Ta basal plane of the $\sqrt{13} \times \sqrt{13}$ structure according to the FT model (Ref. 6). The dashed rhombus denotes the unit cell of the $\sqrt{13} \times \sqrt{13}$ superlattice. (b) Tight-binding calculation of the band structure of the commensurate CDW phase in $1T$ -TaS₂. The different sidebands 1, 2, and 3 are indicated (taken from Ref. 13). (c) Band structure calculation using the full potential linearized augmented-plane-wave (FLAPW) method (Ref. 17) in the framework of the generalized gradient approximation (Ref. 18). The Ta 5d band is shown by the arrow.

and the inherent backfolding of electronic bands due to new zone boundaries. We focus on the band structure at the Γ point. One becomes aware that the band structure consists of three main parts, a band manifold near the Fermi level and two band manifolds consisting of three bands each. The degeneracy of the CDW bands 2 is partly removed near Γ and the calculation predicts one band slightly above 0.4 eV and 2 bands slightly below 0.4 eV. Along high-symmetry directions [off the Γ point; see Fig. 1(b)], the degeneracy is removed and one observes six bands, as expected from the FT model.⁶ The bands near E_F contribute to the lower Hubbard band (LHB). It is this LHB which shifts away from E_F upon cooling below 180 K, whereby opening the energy (pseudo)gap as shown by recent data.^{5,8-12} We note finally that there is no calculation available along the $[\Gamma A]$ direction for the C phase and, consequently, restrict our comparisons to the Γ point.

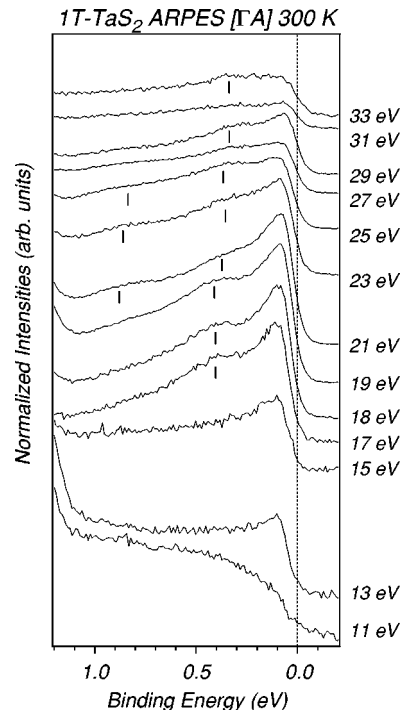


FIG. 2. Normal emission ARPES spectra of $1T$ -TaS₂ taken at 300 K (in the QC phase) along $[\Gamma A]$. The photon energy varies from 11 eV up to 33 eV. The ticks indicate clearly visible sidebands stemming from the CDW-induced $\sqrt{13} \times \sqrt{13}$ superstructure.

Part (c) of Fig. 1 reports a bulk band structure calculation for the undistorted phase, i.e., with no CDW's present. The calculation has been performed using the full potential linearized augmented-plane-wave (FLAPW) method¹⁷ in the framework of the generalized gradient approximation.¹⁸ Further details may be found elsewhere.^{9,19} Two issues need to be addressed. First, the Ta 5d band exhibits a small electron pocket around Γ , for which, however, no experimental proof has been found up to now.⁸⁻¹⁵ Second and more important in this context, is the clear two-dimensional (2D) character of the Ta 5d band (indicated by the arrow) as evident from the nearly dispersionless behavior between A and Γ , i.e., in the perpendicular direction in \mathbf{k} space where we carried out our measurements.

Figure 2 presents our ARPES data, taken at normal emission (along the $[\Gamma A]$ direction) and 300 K for a large range of photon energies from 11 up to 33 eV. This photon energy range reaches from the Γ_2 point to the Γ_3 point, thus covering a little more than one entire Brillouin zone (assuming a work function of 4.5 eV and an inner potential of 10 eV according to Manzke *et al.*¹⁴). The spectra show distinct features as indicated by the ticks, which are not expected from calculations of the unreconstructed lattice presented in Fig. 1(c). This result is in complete agreement with ARPES data already published, which proved already the existence of spectral structures in the band structure between 1 eV binding energy and E_F .⁸⁻¹⁵ The weakness of the features, however, shows that the coherence length of the CDW domains cannot be large in coincidence with STM data.⁵ Therefore measurements must be performed well below 180 K in the C

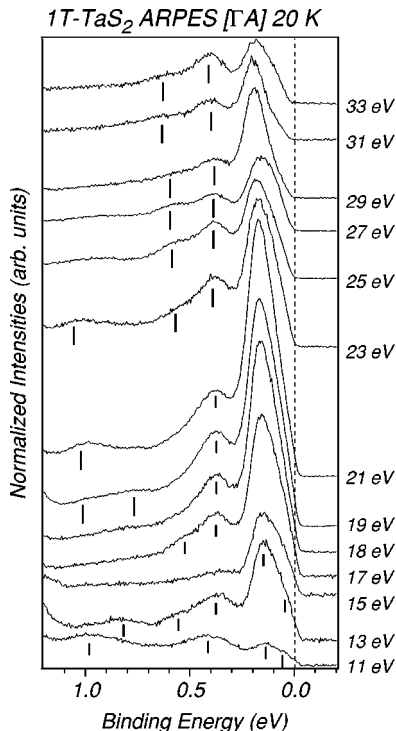


FIG. 3. Normal emission ARPES spectra of 1T-TaS₂ taken at 20 K (in the C phase) along [ΓA]. The photon energy varies from 11 eV up to 33 eV. The ticks indicate clearly visible sidebands stemming from the CDW-induced $\sqrt{13} \times \sqrt{13}$ superstructure.

phase. Finally, we note in, particular, that the strong intensity variations of the satellite peaks observed in Fig. 2 as a function of the photon energy are proof of the considerable influence of photoemission matrix elements. Especially around 20 eV photon energy, the LHB near E_F has a clearly visible intensity maximum. Furthermore, the very small dispersion with $h\nu$ (approximately 50 meV) is of the same order as the \mathbf{k}_\perp dispersion from the calculation of Fig. 1(c) for the non-CDW phase. At low photon energies, a band nearly outside our measurement region becomes apparent. This band stems from the S 3*p* orbitals and is calculated to have a slightly lower binding energy in LDA than in our ARPES data.

Figure 3 displays ARPES spectra taken at normal emission, but now at 20 K, well below the first-order transition at 180 K. One observes a strong intensity pileup around 200 meV corresponding to the LHB. The intensity, especially of this LHB, has a maximum around 21 eV photon energy, which coincides well with the observation in the QC phase (see Fig. 2). In addition, an energy gap is evident from the shift of the whole spectral intensity away from E_F , yet leaving small but finite spectral weight at E_F . The gap magnitude equals 180 meV, taking the maximum binding energy of the LHB. This is in agreement with former values.^{10–12,15} The actual (pseudo)gap value is, however, twice this value, as given by the energy difference between the LHB and UHB, caused by the Coulomb repulsion U_{dd} between the *d*-band electrons.

The finding in this paper is the clear evidence of *more* than three satellite peaks in the C-phase spectra. Up to now, only the three main bands as predicted by the standard FT

model have been found, although Manzke *et al.*¹⁴ reported a fourth peak around 1 eV in ARPES spectra taken with 21.2 eV photons near Γ . We evidence the existence of at least six different CDW-induced peaks, which we shall consider in the following. For spectra at 11, 19, 21, and 23 eV photon energy, a bump at 1 eV binding energy is evident. Furthermore, spectra taken at 13 and 19 eV prove the existence of a second faint shoulder around 0.8 eV. Much more pronounced, however, are the split peaks around 0.45 eV. Whereas the 11 eV spectrum reveals one broad peak centered at 0.4 eV, this broad peak splits off into 2 at approximately 0.55 and 0.38 eV. The splitting of these peaks stays evident for all photon energies, whereby the 25 eV spectrum exhibits also a very distinct splitting.

What concerns the sidebands 2 and 3 (i.e., six bands in total), we can say that the coincidence of our data shown in Fig. 2 and Fig. 3 with the calculation of Smith *et al.*¹³ for the C phase [see Fig. 1(b)] is very good. We observe the removal of the degeneracies of the sidebands 2 and even find evidence for a removal of the degeneracy of the bands 3 (Fig. 3) along [ΓA]. As a consequence, we can, at a first glance, assign our observed fine structure to the symmetry modifications induced by the $\sqrt{13} \times \sqrt{13}$ superstructure in the C phase. This result yields further evidence for the correctness of the Fazekas-Tosatti model.

Surprisingly, the LHB with its maximum at 180 meV shows a slightly asymmetric edge towards the Fermi level; even a distinct shoulder is observable especially in the spectra at 13 and 15, but also at 31 eV. From this observation, one might get the impression that even the LHB consists of two differently contributing peaks. However, concerning the strongly correlated nature of the initial Ta 5*d* electrons, the origin of such a splitting as observed in our low-temperature data is not clear. The FT model, predicting one electron sitting in the star center, can *a priori* not account for that observation. Possible explanations may be the following: (i) Photoemission with an average escape depth of approximately 10 Å should in fact probe not only the first Ta plane under the chalcogen plane exposed upon cleavage. Also the second Ta plane lying deeper in the sandwiches may be accessible with these photon energies, as the distance from the surface to the second Ta plane is only about 9 Å. If this second Ta plane now exhibits an in-plane CDW with a different rotation with respect to the chalcogen planes, one would expect to receive two different sets of CDW-induced spectral features with different symmetries. Then, however, our experimentally found six peaks could also correspond to two sets of three peaks stemming from each Ta plane. We cannot rule out this possibility. (ii) An interesting alternative might also be spin-orbit-split Ta 5*d* states, but to our knowledge, spin-orbit splitting has not been observed up to now in similar compounds containing Ta. The nature of the observed fine structure remains thus somehow uncertain and theoretical input is highly desired. Finally we note that the observed bands show nearly no dispersion, explained by the localized character of the electrons, residing in the Ta atom clusters in the commensurate phase.⁶ This emphasizes the 2D character of the bands and the lack of 3D interaction for the [ΓA] direction perpendicular to the sheets. As a consequence,

more detailed band structure information of the C phase is essential and strongly desired to further consider the low-temperature band structure of 1T-TaS₂.

Using high-resolution angle-resolved photoemission spectroscopy, we were able to show that normal emission spectra of the C phase reveal evidence for a fine structure in the CDW-induced features between 1 eV binding energy and the Fermi level, being predicted by a tight-binding calculation. We observe up to six different peaks. This fine structure may be explained by the subband manifold of the Ta 5d band,

split off due to the CDW-induced $\sqrt{13} \times \sqrt{13}$ superstructure and, hence, coincides with the Fazekas-Tosatti model. An asymmetric LHB, as is found, does not fit into that picture. The spectra show further the clear 2D character of the Ta 5d band derived manifolds along $[\Gamma A]$ and a considerable influence of matrix element effects.

This work has been supported by the Fonds National Suisse pour la Recherche Scientifique.

*Corresponding author. Present address: Institut de Physique, Université de Neuchâtel, CH-2000 Neuchâtel, Switzerland. Electronic address: thorsten.pillo@unine.ch

¹J.A. Wilson and A.D. Yoffe, *Adv. Phys.* **18**, 193 (1969).

²J.A. Wilson, F.J. Di Salvo, and S. Mahajan, *Phys. Rev. Lett.* **32**, 882 (1974).

³J.A. Wilson, F.J. Di Salvo, and S. Mahajan, *Adv. Phys.* **24**, 117 (1975).

⁴M. Grioni and J. Voit, in *Electron Spectroscopies Applied to Low-Dimensional Materials*, edited by H. Starnberg and H. Hughes (Kluwer, Dordrecht, 2000).

⁵X. Wu *et al.*, *Science* **243**, 1703 (1989); B. Giambattista *et al.*, *Phys. Rev. B* **41**, 10 082 (1990); W. Han *et al.*, *ibid.* **48**, 8466 (1993); B. Burk *et al.*, *Phys. Rev. Lett.* **66**, 3040 (1991); X. Wu *et al.*, *ibid.* **64**, 1150 (1990).

⁶P. Fazekas and E. Tosatti, *Philos. Mag. B* **39**, 229 (1979); *Physica B* **99**, 183 (1980).

⁷N. F. Mott, *Metal-Insulator Transition* (Taylor & Francis, London, 1990), p. 138; F. Gebhard, *The Mott Metal-Insulator Transition*, Springer Tracts in Modern Physics Vol. 137 (Springer, New York, 1997).

⁸Th. Pillo, J. Hayoz, H. Berger, M. Grioni, L. Schlapbach, and P. Aebi, *Phys. Rev. Lett.* **83**, 3494 (1999).

⁹Th. Pillo, J. Hayoz, H. Berger, R. Fasel, L. Schlapbach, and P.

Aebi, *Phys. Rev. B* **62**, 4277 (2000).

¹⁰B. Dardel, M. Grioni, D. Malterre, P. Weibel, Y. Baer, and F. Lévy, *Phys. Rev. B* **45**, 1462 (1992).

¹¹B. Dardel, M. Grioni, D. Malterre, P. Weibel, Y. Baer, and F. Lévy, *Phys. Rev. B* **46**, 7407 (1992).

¹²F. Zwick, H. Berger, I. Vobornik, G. Margaritondo, L. Forró, C. Beeli, M. Onellion, G. Panaccione, A. Taleb-Ibrahimi, and M. Grioni, *Phys. Rev. Lett.* **81**, 1058 (1998).

¹³N.V. Smith, S.D. Kevan, and F.J. Di Salvo, *J. Phys. C* **18**, 3175 (1985).

¹⁴R. Manzke, O. Anderson, and M. Skibowski, *J. Phys. C* **21**, 2399 (1988).

¹⁵R. Manzke, T. Buslaps, B. Pfalzgraf, M. Skibowski, and O. Anderson, *Europhys. Lett.* **8**, 195 (1989).

¹⁶H. Berger (unpublished).

¹⁷P. Blaha, K. Schwarz, and J. Juitz, computer code WIEN97, Vienna University of Technology [improved and updated UNIX version of the original copyrighted WIEN code, published by P. Blaha, K. Schwarz, P. Sorantin, and S. B. Trickey, *Comput. Phys. Commun.* **59**, 399 (1990)].

¹⁸J.P. Perdew, K. Burke, and M. Ernzerhof, *Phys. Rev. Lett.* **77**, 3865 (1996).

¹⁹P. Aebi, Th. Pillo, H. Berger, and F. Lévy, *J. Electron Spectrosc. Relat. Phenom.* **117-118**, 433 (2001).